MOF Catalysts for Plastic Depolymerization

Bao-Nguyen T. Nguyen,[a] Tristan T. Y. Tan,[a] Ken-ichi Otake,[a,b] Susumu Kitagawa*[a,b] and Jason Y. C. Lim*[a,c]

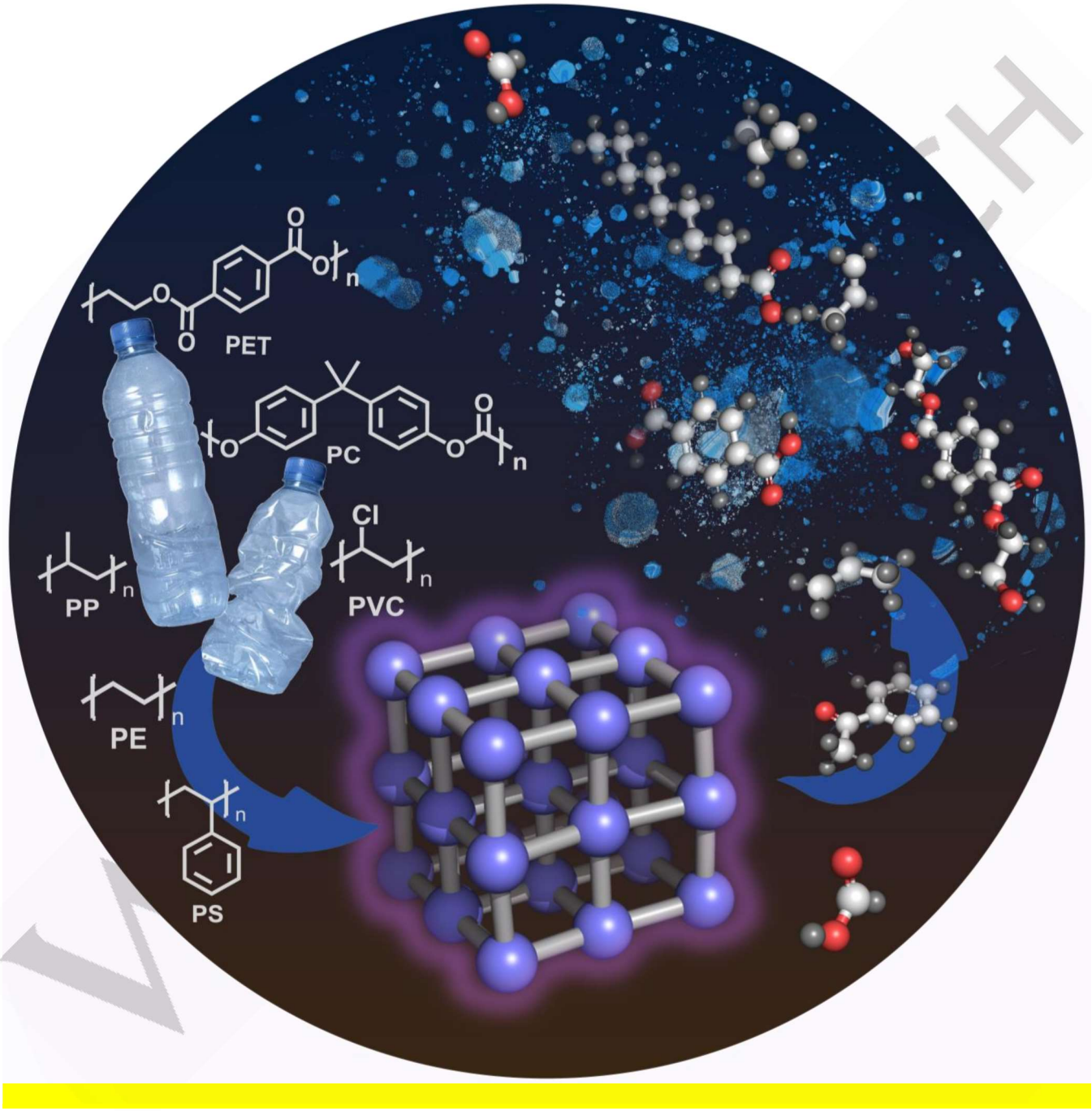

[a] Dr. B-N.T. Nguyen, Dr. T.T.Y. Tan, Prof (Dr.) K.-i. Otake, Prof (Dr.) S. Kitagawa, Prof (Dr.) J.Y.C. Lim
Laboratory of Green Porous Materials, Institute of Materials Research and Engineering (IMRE)
Agency for Science, Technology and Research (A*STAR)
2 Fusionopolis Way, Innovis #08-03, Singapore 138634, Republic of Singapore
E-mail: jason_lim@imre.a-star.edu.sg
[b] Prof (Dr.) K.-i. Otake, Prof (Dr.) S. Kitagawa
Institute for Integrated Cell-Material Sciences, Kyoto University
Institute for Advanced Study, Kyoto University
Yoshida, Ushinomiya-cho, Sakyo-ku, Kyoto, 606-8501, Japan
Email: kitagawa@icems.kyoto-u.ac.jp
[c] Prof (Dr.) J.Y.C. Lim
Department of Materials Science and Engineering
National University of Singapore (NUS)
9 Engineering Drive, Singapore 117576, Republic of Singapore

Abstract: Depolymerization is a promising solution to address the escalating global plastic waste crisis, as a key enabler for emerging technologies in chemical upcycling and closed-loop recycling of plastics. By virtue of their unparalleled bottom-up designability for structural control, stability, reactivity and compatibility with catalytically-active metal nanoparticles and enzymes, MOFs have enormous potential as an emerging class of porous heterogeneous catalysts for plastics depolymerization. Herein, we highlight key considerations and advances in MOF catalyst development and design for a range of depolymerization reactions, including alcoholysis, hydrogenolysis, pyrolysis, photocatalytic oxidation and enzymatic hydrolysis. Other than enabling MOFs to efficiently depolymerize the most abundant plastics in production today, including those with unreacted C-C backbones (e.g. polyolefins) and polymers with cleavable backbone linkages (e.g. polyesters), their versatility also extends to emerging applications in microplastic capture and degradation from wastewater. These unique properties of MOFs position them as potentially scalable and reusable heterogeneous catalysts that can complement existing inorganic catalysts for practical depolymerization.

1. Introduction

Plastics are synthetic polymers which have revolutionized modern society since their industrial production, due to their exceptional versatility as low-cost materials. However, despite these transformative benefits, plastics have also contributed to a global crisis, particularly in waste management. This is largely due to their predominately linear life cycles which lead to accumulation of tremendous quantities of waste, with much of it accumulating in landfills or in the environment. This has resulted in severe ecological damage, disrupting natural habitats and introducing microplastics into the food chains. Alternatively, discarded plastics are burned in incinerators, releasing greenhouse gases and exacerbating climate change. While recycling is intended to reduce these problems by transitioning plastics into a circular lifecycle, only a small fraction of plastics is being recycled mechanically, largely limited to PET and HDPE. Although this is set to increase following legislative mandates, mechanical recycling has inherent limitations due to inevitable material degradation over repeated cycles that compromises their properties and applications.[1] Thus, mechanically recycled plastics eventually face disposal. With more than 350 million tonnes of plastics produced annually, a figure projected to further increase in the foreseeable future,[2] new strategies to address plastics' unsustainable end-of-life are urgently needed. One of the most promising strategies is depolymerization, identified by the IUPAC in 2023 as amongst the Top Ten Emerging Technologies in Chemistry.[3] Here, long-chain polymers are chemically broken down into monomers that can be reconstituted into virgin polymers (i.e. closed-loop chemical recycling), or can be converted into other small molecules of industrial importance with higher economic value (i.e. upcycling),[4] reducing societal reliance on non-renewable petroleum feedstock for their production. Several forms of depolymerization are technologically mature at the time of writing, including PET chemical recycling and plastic pyrolysis, with several facilities already operational to treat plastic waste in multitonne-scales annually.[5] While catalysts are essential in these processes, there is much potential for further catalyst development to reduce energy demands, improve product selectivity and even produce new classes of products altogether.

Depolymerisation can be catalysed by a range of homogeneous and heterogeneous catalysts (metal salts, complexes and organocatalysts)[6] and heterogeneous catalysts (porous zeolites[7], silica- and carbon-supported catalysts[8]). While homogeneous systems offer bottom-up designability, they are often difficult to recover and reuse, which limits their sustainability in practical applications. Heterogeneous catalysts, including zeolites, metal oxides, silica- and carbon-supported species, and biomass-derived materials, are generally preferred for their ease of separation, thermal robustness, and reusability. Zeolites, in particular, stand out as the traditional choice in high-temperature processes such as pyrolysis and glycolysis due to their unparalleled thermal robustness and Brønsted acidity, which enable efficient cleavage of plastic polymers.[7, 9] Nonetheless, there is increased emphases on achieving high product selectivity and narrow, controllable product distributions, together with greater diversification of products from limited feedstock composition (e.g. hydrocarbon polyolefins) that require specific catalytic capabilities such as oxidation and hydrogenolysis. These requirements call for highly-designable heterogeneous catalysts that can be tailored for different reactions, yet maintain sufficient thermal stability for ease of recovery and reuse. In this regard, MOFs, distinct from zeolites, have emerged as a complementary

class of porous materials, offering unique advantages in the area of depolymerization, whilst providing a versatile platform for catalytic processes that include pyrolysis and extend to other transformations.

Compared to zeolites, MOFs have unparalleled bottom-up designability, enabling systematic tailoring of their properties through various strategies. A key concept in MOF design is reticular synthesis,[10] where the pore size can be expanded systematically by increasing the length of the organic linkers, which can directly influences the products' molecular weight distribution[11]. Further, the pore chemistry can be modified by introducing functional groups on the linkers or substituting different metals in the MOF nodes, thereby altering their catalytic properties while maintaining the same underlying network topology [10]. In contrast, altering the pore size of zeolites often necessitates changes to the network topology, effectively creating a new zeolite with distinct reactivity, a process heavily reliant on trial-and-error approaches. In addition, the current fourth generation of MOFs incorporates advanced concepts such as defects and disorder to enhance catalytic performance[12], where controlled defect engineering improves reactivity and accessibility within the material,[13] and hybrid approaches that integrate other functional materials, such as enzymes, semiconductor components, or metal nanoparticles, extending the utility of MOFs in complex catalytic systems. These innovations are particularly relevant for advanced catalysis, where precise control over reaction mechanisms, product distribution, lower reaction temperatures, and photocatalytic capabilities are critical.

Herein, we showcase how the designability of MOFs can be exploited to catalyse depolymerization of a large variety of high-volume plastics, via a range of reactions that include glycolysis, hydrogenolysis, pyrolysis, photocatalytic oxidation and enzymatic hydrolysis. After highlighting important general considerations that should be taken into account for designing and selecting MOFs for depolymerization reactions, we then discuss how MOFs have been utilized for different types of reactions in detail. Not only can MOFs be utilized for bulk depolymerization, they can also be used for capture and in-situ degradation of micro/nano-plastics for wastewater remediation. Finally, we will conclude with a discussion of critical areas for future development of MOF catalysts for this rapidly advancing field.

Susumu Kitagawa obtained a Ph.D. degree from Kyoto University. He is now a Distinguished Professor at the Institute for Integrated Cell-Material Sciences and has been Executive Vice-President of Kyoto University since 2024. He pioneered the science and technology of PCPs and MOFs. He has also discovered and developed their unique structures and functions classified as soft porous crystals

Jason Lim obtained a DPhil in Inorganic Chemistry from the University of Oxford, U.K. He is a Group Leader at the Institute of Materials Research and Engineering. His research interests centre around sustainable catalysis for upcycling and depolymerisation of plastics, porous materials for sustainability applications and functional therapeutic biomaterials. His team has developed numerous strategies for upcycling post-use plastics into functional polymeric materials and industrially-relevant small molecules.

Author Portrait

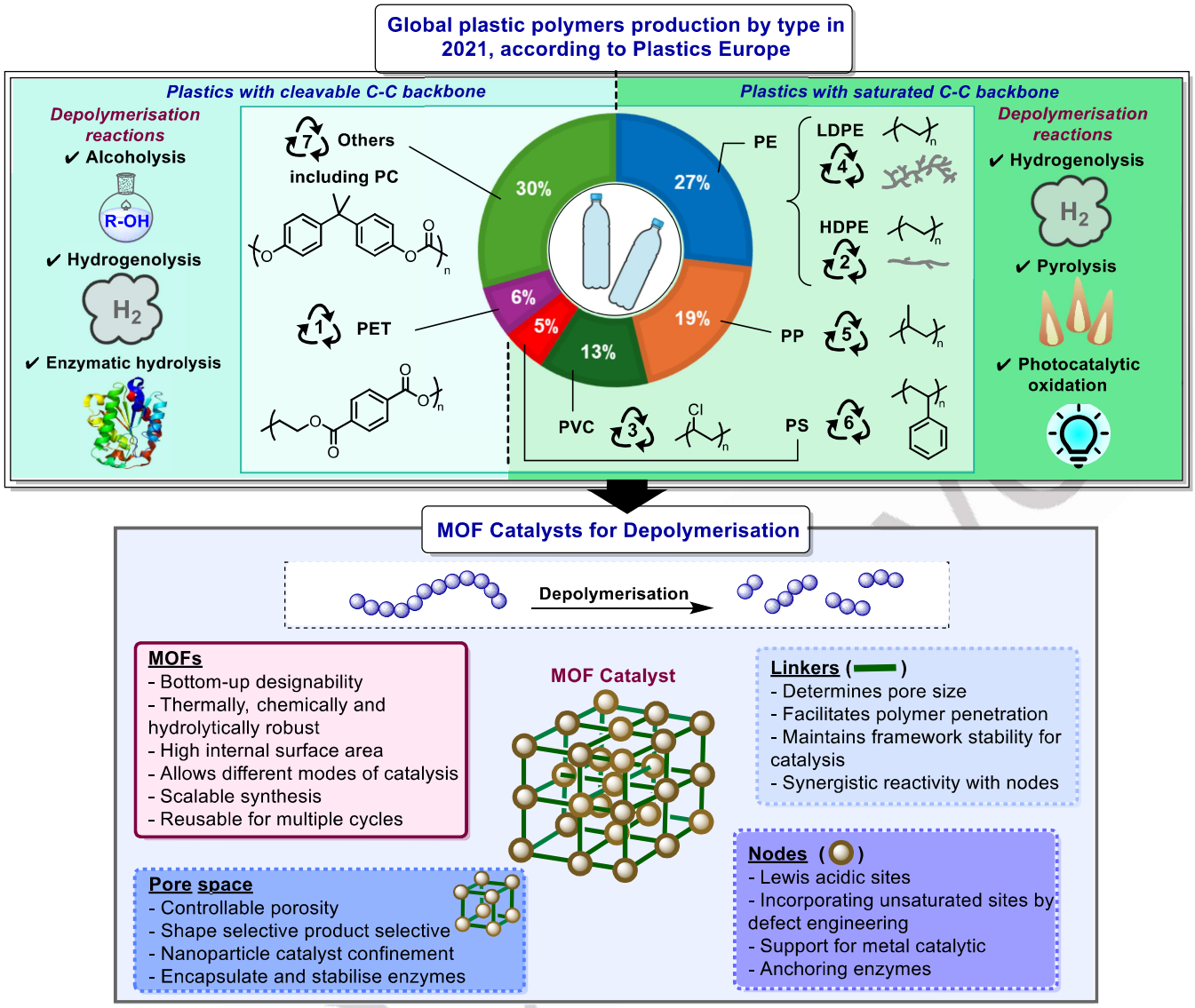

Figure 1. Global plastic production by type in 2021, according to Plastics Europe[14] with respectively depolymerization strategies, and MOFs as emerging catalysts for chain depolymerization.

2. General Considerations

The main varieties of plastics produced on commercial scales can be broadly grouped into two main classes: (1) those containing saturated C-C backbones (e.g. polyolefins, PS, PVC) and (2) those with heteroatom-containing backbone linkages (e.g. polyesters, polyamides, polycarbonates, polyurethanes) Strategies adopted to depolymerize these plastics using MOFs thus differ accordingly. For the former class of polymers, the inherent chemical inertness of the polymer backbone often requires metal-catalyzed activation, such as via σ-bond metathesis reactions at elevated temperatures, for chain scission to occur.[15] Hence, MOF catalysts designed for such reaction prominently feature accessible metal centers, either via coordinatively-unsaturated sites on the nodes by topological design or by inclusion of missing linker defects, or through inclusion of supported metal complexes or nanoparticles. The rigidity of the framework prevents the reactive metals from aggregating, ensuring their activity and stability. For the latter class, the cleavable bonds make them susceptible to nucleophilic attack that cleaves the polymer chains, hence metal node acidity and organic linker basicity can work synergistically to activate the polymer and reagent (e.g. alcohols) respectively to facilitate nucleophilic cleavage. For instance, this synergistic catalysis is exploited in polycarbonate methanolysis catalysed by ZIF-8 ($[Zn(MeIm)_2]$, MeIm = 2-methylimidazolate) (vide infra).[16] Additionally, MOFs can act as supports or nanoreactors that stabilize enzymes within their pores to augment biocatalytic polyester hydrolysis. Table 1 summarizes key reaction parameters and outcomes when MOFs are used in depolymerization of different varieties of plastics.

Table 1. Summary of MOF Catalysts for Depolymerisation of Plastics.

Reactions	Plastics	MOF	Reaction conditions	MOF catalyst loading	Reaction Outcome	MOF Reusability	Ref
Glycolysis	PET	ZIF-8	180 °C, 4 h, ambient pressure	1 wt% w.r.t. PET	88.2% PET conversion, 65.9% BHET yield	-	[17]
		Dual-porous ZIF-8 nanoparticles w mesopores			91.7% PET conversion, 76.1% BHET yield	-	
		ZIF-8	197 °C, 1.5 h, ambient pressure		100% PET conversion, 76.75% BHET yield	3 times with negligible change in catalytic activity and reaction outcome.	[18]
		MAF-6	180 °C, 4 h, ambient pressure	1 wt% w.r.t. PET (15.33% Zn content)	92.4% PET conversion, 81.7% BHET yield	5 times, product yield drops to 71.2%	[19]
		MAF-5		1.78 wt% w.r.t. PET (8.55% Zn content)	72.3% PET conversion, 39.0% BHET yield	-	
Methanolysis	BPA-PC	MAF-6	130 °C, 3 h, autogenous pressure in autoclave	5 wt% w.r.t. PC	98.6% PC conversion, 86% BPA yield	-	[16]
		ZIF-8			95.9% PC conversion, 94.1% BPA yield	3 times with 18% drop in PC conversion and 21.9% drop in BPA yield	
		MOF-5-ethylenediamine			97.3% PC conversion, 99.2% BPA yield	3 times with 13.9% drop PC conversion and 32% drop in BPA yield	
Hydrogenolysis	PE	UiO-66-RuH_2	200 °C, 72 h, 35 bar H_2	1 wt% w.r.t. PE, (4 µmol of Ru)	90% PE conversion, 58% liquid alkanes selectivity.	-	[11]
		UiO-67-RuH_2		1.1 wt% w.r.t. PE, (4 µmol of Ru)	78% liquid alkanes selectivity	5 times, no significant drop in catalytic activity and selectivity	
		UiO-68-RuH_2		1.4 wt% w.r.t. PE, (4µmol of Ru)	94% liquid alkanes selectivity	-	
		DUT-5-RuH_2	200 °C, 20 h, 30 bar H_2	2 wt% w.r.t. PE, (33 µmol of Ru)	80% PE conversion, 83%liquid alkane selectivity	4 times with minimal loss of activity (17% loss in liquid product yield)	[20]
	PET	UiO-66 transforms to MIL-140A during reaction	260 °C, 24 h 1 atm H_2	5 mol%	98% yield (72% terephthalic acid, 26% monomethyl Terephthalate)	4 times, total product yield drops to 74%	[21]
Pyrolysis	LDPE	UiO-66	400 °C, 5h, under Ar	10 wt% w.r.t. plastic	76.9% conversion, 44.4% liquid and 32.4% gas yield	-	[13]
	HDPE				80.7% conversion, 51% liquid and 29.7% gas yield	2 effective cycles, drop to 48.7% conversion on 3rd cycle	
Photo-catalyst	PLA	ZnO/UiO-66-NH_2	25 °C, 300 W Xe lamp, 21 A, 14 V, distance 5 cm, bulb window 25.4 mm, full light spectrum, air, ambient pressure	10 wt% w.r.t. plastic	conversion rate 57.10 mg/g_{cat}·h, 14.4% acetic acid yield 91.6% acetic acid selectivity	4 cycles with minimal change in product yield	[22]
	PVC			10 wt% w.r.t. plastic	conversion rate 21.4 mg/g_{cat}·h, 9.2% acetic acid yield	-	

					91.6% acetic acid selectivity		
	PVC	CDs/Zr-MOF	300 W Xe lamp, 21 A, distance 10 cm, full light spectrum, air, ambient temperature	1 g photocatalyst per 0.2 g PVC, 10% mass fraction of CDs in the composite	76.5% plastic conversion,14% acetic acid yield, production rate 0.17 mg/g_{cat}·h	5 cycles with minimal change in conversion rate	[23]
Enzyme hydrolysis	PET Film (Mw = 24000 and 36000)	CrL_ UiO-66-NH_2	Room temp., stirring 400 rpm, 24h	20 mg catalyst per cm^2 plastic film	1.68-2.52% PET degradation Mw= 24,000 and 36,000 respectively	-	[24]
	PET	HiC@NU-1000	pH 7.5, 80 °C, 48h	5mg catalyst with 0.016 µmol HiC per 5.2 mg PET	47% terephthalic acid yield, 14% BHET yield	-	[25]
		MC@CaZn-MOF	pH 8.0, 60 °C, 5 days	10 nm enzyme concentration,	96% plastic conversion, 9.5 mM TPA, ~100% selectivity	5 cycles with 62.1% catalytic activity retained	[26]

These reactions are typically performed at high temperatures, almost always exceeding 180 °C (Table 1), and/or generation of reactive intermediates (e.g. alkoxides), hence the MOF catalysts should have sufficient thermal and chemical stability. Furthermore, in depolymerization of polyesters, acids (e.g. terephthalic acid [TA] from PET) are produced, which can potentially lead to ligand exchange with the MOF and alter their reactivity. During the hydrogenolysis of PET by UiO-66 ([Zr6O4(OH)4(BDC)6], BDC = 1,4-benzenedicarboxylate), for instance, ligand exchange leads to conversion of the MOF to the less porous MIL-140A [ZrO(BDC)] with reduced activity.[27] On the other hand, although enzyme-mediated biocatalysis occurs at much lower temperatures, these reactions typically occur in the presence of salts and at slightly basic pH, necessitating that the MOFs used are hydrolytically stable and tolerant to these conditions.

Enhancing the thermal, chemical and hydrolytic stability of MOFs is an active area of research, with key insights summarized in recent reviews.[28] The stability of MOFs generally increases with greater linker rigidity, strength of metal-linker coordination, and framework connectivity. Generally, such MOFs contain highly charge-dense metals (e.g. Zr^{4+}, Cr^{3+}, Al^{3+}) with strongly-coordinating multivalent linkers possessing rigid aromatic cores. While coordinatively-unsaturated catalytically-active metal centres can facilitate depolymerization, these can compromise on MOF stability by weakening the framework structure if generated through missing linker or missing cluster defects. Table 2 summarises the decomposition temperatures of common MOFs employed in depolymerization reactions, determined by TGA. Although this technique is extremely valuable for assessing MOF thermal stability, several limitations have been noted[28b], including the heating rate and atmosphere, the inability to detect changes without mass loss such as phase transitions, and difficulty in distinguishing the plateau region from decomposition in thermograms. Thus, assessment of MOF tolerance need to be performed for different depolymerization reactions, to understand the origins of observed catalytic behaviour and potential catalyst reusability.

Table 2. Decomposition temperature of MOFs used in depolymerization.

MOFs	T_d / °C	MOFs	T_d / °C
UiO-66, UiO-67	500[29] under N_2	MAF-5, MAF-6, MAF-32	<400[8] under N_2
Cu-BTC	300[30] under N_2	NU-1000	500[31] under N_2
Zn-BTC	450[30] under N_2	ZIF-8	600[9] under N2

Accessibility to catalytically-active sites is a key parameter affecting catalytic activity. MOF porosity potentially provides large internal surface area for reactivity, but this requires effective penetration of polymers into the pores, which is largely dictated by polymer molecular weights, sterics and topology (linear vs branched). Despite being entropically unfavourable, polymer penetration can occur both in the solution state or in the melt state, via diffusion-dominated processes with enthalpic contributions from non-covalent interactions between the polymers and MOF nanochannels.[32] Evidence of penetration can be obtained from DSC experiments: As infiltrated polymers do not contribute to the phase transition enthalpies of the bulk polymers, increasing extents of penetration results in measurable decrease in enthalpy upon successive DSC cycles.[32-33] Additionally, 2D solid-state NMR (e.g. ^{1}H DQ/ ^{1}H SQ homonuclear correlation) experiments can reveal through-space interactions arising from short contacts between polymers and the organic MOF linkers that indicate polymer entry into the pores. Using these experiments, HDPE has been shown to penetrate the pores of UiO-66 MOFs at 350 °C,

but not the extensively-branched LDPE.[13] Even if the polymers can infiltrate the MOFs, the pores must still be sufficiently large to ensure that the transition states for polymer scissions within the confined pores must still be sterically accessible. On the other hand, polymers containing bulkier aromatic groups (e.g. PET, bisphenol-A polycarbonates) are unlikely to penetrate the pores of MOF catalysts currently employed for alcoholysis (e.g. ZIF-8), thus it is more likely that reactions occur on the MOF exterior in contact with exposed catalytic sites.[16] While employing MOFs with larger pore windows is a possible strategy, Chi and Lee demonstrated an alternative approach using ZIF-8 nanoparticle aggregates which contain mesopores for PET glycolysis. These dual-pore catalysts was shown to enhance glycolysis efficiency compared to ZIF-8 alone, (Table 1, entry 1) attributed to enhanced interfacial contact sites between Zn^{2+} centres and PET that facilitate PET scission.[17]

A key advantage of heterogeneous catalysts over homogeneous catalysts is their ease of recovery and reuse for multiple iterations of depolymerization. For MOFs to be reusable, they must not only be tolerant to the reaction conditions as aforementioned, but also maintain accessibility to reactive sites to retain their catalytic activity over multiple reaction cycles. Depolymerisation can sometimes lead to accumulation of shorter chain oligomer products or reaction by-products within MOF pores that reduces catalyst porosity and lead to catalyst deactivation, as observed from UiO-66-catalysed polyolefin pyrolysis[13] and ZIF-8-mediated polycarbonate methanolysis.[16] The integrity of MOF catalysts after successive reactions can be assessed through XRD, with peak broadening indicative of crystallite size changes, appearance of new peaks suggesting phase transitions, and broadened baselines suggesting MOF decomposition or accumulation of amorphous material. Further evidence can be sought from TEM imaging, which can show changes in crystal morphology: the phase transition from UiO-66 to MIL-140-A during the aforementioned PET hydrogenolysis was seen from change in MOF morphology from octahedra to rods.[27]

Considering the massive scale of plastic waste production, the MOF catalysts chosen should be feasible for large-scale synthesis at low cost. In this regard, archetypical MOFs comprising of abundant and inexpensive metals and linkers (e.g. TA), with established industrial-scale syntheses (e.g. UiO-66, ZIF-8),[34] have been the focus of most studies on depolymerization (Table 1). The following sections will consider each class of MOF-catalysed depolymerization reaction in greater detail.

3. Depolymerization of Plastics

3.1. Alcoholysis

Alcoholysis is one of the leading methods for depolymerization of plastics containing cleavable backbone linkages (e.g. esters, carbonates, urethanes), and can be catalysed by inorganic salts (e.g. zinc acetate) and organic bases (e.g. DBU).[35] PET, the most-produced polyester, can be depolymerized by glycolysis using ethylene glycol to generate bis(2-hydroxyethyl) terephthalate (BHET), which is industrially-valuable as a precursor for synthesis of foams, resins and coatings, and is also an important intermediate in chemical recycling of PET.[36]

The first example of MOF-catalysed PET glycolysis was reported by Suo in 2017[18] using ZIF-8 to depolymerise PET into BHET and its dimer. This was largely mediated by the acidity of the Zn nodes, which polarizes the PET C=O bonds and activates them towards nucleophilic attack (Fig. 2A). The role of metal acidity for PET glycolysis efficiency was subsequently demonstrated using M-BDC MOFs (M = Zn, Ni, Cu).[37] Zn-BDC, which was most Lewis acidic, gave the highest rate of glycolysis, with activity decreasing in the order Zn > Ni > Cu, correlating with MOF Lewis acidity as determined by NH_3 TPD experiments. As the small pore size of ZIF-8 (11.6 Å) restricts entry of PET fragments to access the catalytically-active Zn^{2+} centres within the MOF pores, Yang et. al. showed that MAF-6 (RHO-[Zn(eim)2], eim = ethylimidazolate) with larger pore size (16.7 Å) was able to elicit excellent BHET yields (81.7%) after glycolysis.[19] The authors propose that partial glycolysis first occurs on the MOF surface, producing fragments such as BHET dimers that can enter the MOF pores for further glycolysis to form BHET (Fig. 2B). The related MAF-5 (ANA-$[Zn(EtIm)_2]$, pore diameter 11.6 Å) was found to give much lower BHET yields compared to MAF-6 (Table 1). Although MOFs alone can effectively catalyse glycolysis reactions, Chen showed that nanoparticle composites of $CoFe_2O_4$ and ZIF-8/ ZIF-67 could improve the BHET conversions compared to just using the MOFs alone.[38]

Previous reports on heterogeneous catalysts for PET glycolysis, including those based on silica and metal oxides,[35] typically require very high reaction temperatures in the range of 260 to 300 °C. This is largely due to the low mobility of PET, which necessitates elevated temperatures to enable effective interaction with solid catalysts. In contrast, the MOF-based catalysts discussed herein achieve high BHET yields at approximately 190 °C under ambient pressure. This level of performance is comparable to that of benchmark homogeneous catalysts such as zinc acetate,[35, 39] suggesting that MOFs can deliver homogeneous-like reactivity while retaining the advantages of solid-state systems. However, partial dissolution of metal ions, particularly from ZIFs, cannot be ruled out under glycolysis conditions. Post-reaction analyses for metal leaching are therefore essential to confirm catalyst stability. For example, in the case of MAF-6, ICP-MS analysis revealed that 3.7% of metal ions leached out after five recycling cycles.[19] These findings highlight the importance of evaluating long-term stability and suggest that there remains significant potential to develop more chemically robust MOFs with improved durability under glycolysis conditions.

Similar to polyesters, polycarbonates (PCs) can also be depolymerized via alcoholysis. Although bisphenol-A (BPA)-PCs are valued for their excellent impact resistance and optical clarity, the health concerns of BPA as a potential endocrine disruptor[40] has spurred advances in BPA-PC closed-loop recycling. Like PET, ZIF-8 and MAF-6 can catalyse BPA-PC methanolysis to afford excellent yields of BPA.[16] This was proposed to result from synergistic effects of Zn^{2+} nodes and the basic imidazole linkers: the former activating the carbonate C=O bonds for nucleophilic attack, whilst the imidazole units polarize the methanol O-H bonds to enhance its nucleophilicity (Fig 2C). The authors further demonstrated the important role played by synergistic acid-base catalysis, where MOF-5 $[Zn_4O(BDC)_3]$ post-synthetically modified with ethylenediamine (ED) elicited 97% PC conversion, compared to only 17% for unmodified MOF-5. Despite their efficacy, ZIF-8, MAF-6 and MOF-5-ED showed reduction in activity after 3 cycles of reuse, likely due to pore clogging, MOF agglomeration and leaching of ED from MOF-5-ED.

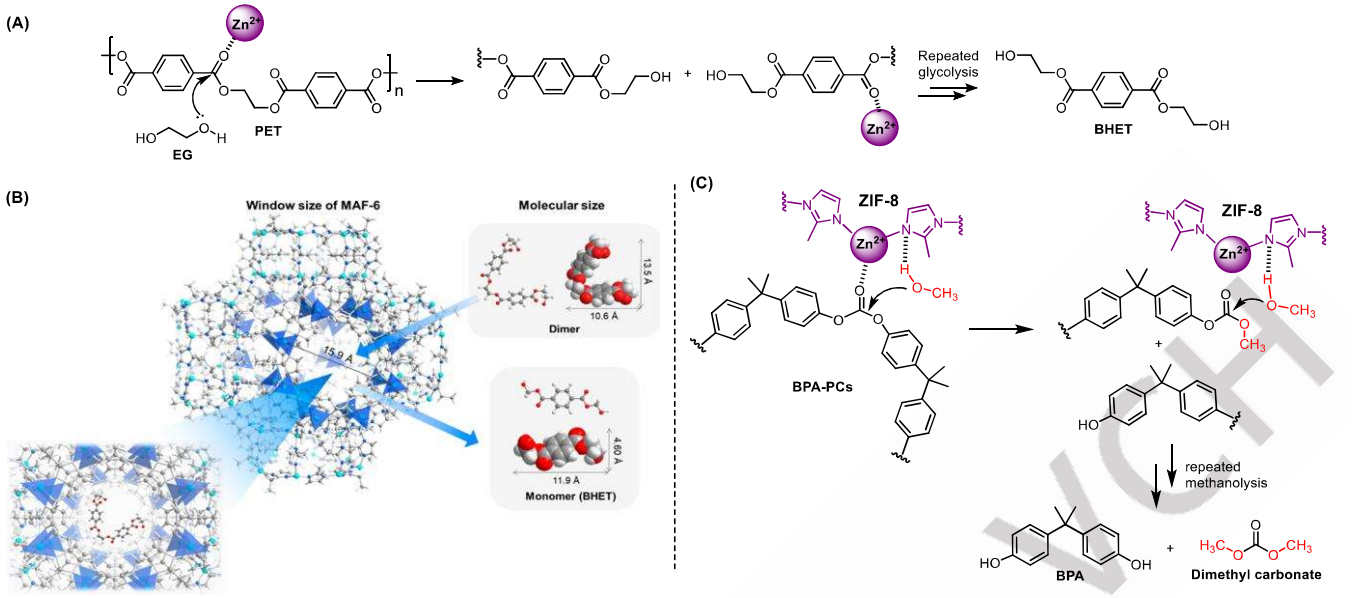

Figure 2. (A) Proposed mechanism of ZIF-8-catalysed PET glycolysis mediated by Zn^{2+} nodes[18]; (B) Dimensions of MAF-6 pore, BHET and its dimer, showing the possibility of glycolysis occurring within the MOF pores. Reprinted with permission from reference[19], copyright (2021) American Chemical Society; (C) Synergistic effects of ZIF-8 node and linkers for PC methanolysis.[16]

3.2. Hydrogenolysis

Hydrogenolysis is attractive for converting polyolefins, which make up nearly 50% of all plastic waste produced, into short- and medium-chain alkanes under relatively mild conditions. Typically, such reactions are catalysed by noble metals (e.g. Ru, Pt) on solid inorganic supports under solvent-free conditions and elevated H_2 pressures.[41] Although high metal loadings are often required, with non-uniform distribution of these catalytic sites resulting in random C-C scission that affect product selectivity, more recent studies have shown that controllable product distributions can be obtained through shape-selective hydrogenolysis where these metal sites are embedded within confined pore spaces.[42] Building on this concept, Manna and coworkers demonstrated that ruthenium dihydrides supported on the nodes of isoreticular series of Zr-based (UiO-66, UiO-67 $[Zr_6O_4(OH)_4(BPDC)_6]$, BPDC = 4,4′-biphenyldicarboxylate, UiO-68 $[Zr_6O_4(OH)_4(TPDC)_6]$, TPDC = ([1,1′:4′,1″-terphenyl]-4,4″-dicarboxylate,)[11] and Al-based MOFs (DUT-5 [Al(OH)(bpdc)], bpdc = 4,4′-biphenyldicarboxylate and MIL-53 [(Al(OH)(bdc)])[20] can efficiently convert PEs into fuel-grade alkanes at 200 °C, with high selectivity for liquid over gaseous alkanes. The catalytically-active RuH_2 species are mounted onto the MOF nodes by post-synthetic metalation reactions.

The authors observed a systematic change in product distribution across isoreticular MOFs with different pore sizes: smaller-pore MOFs yielded higher fractions of gaseous (C1-C4) products and shorter liquid-range alkanes, while larger-pore MOFs produced longer-chain alkanes with broader distributions, along with lower gas yields (Fig. 3A). This size selectivity suggests that catalysis occurs within the MOF pores and is influenced by pore confinement, rather than on degraded frameworks or externally supported species. Supporting this interpretation, control experiments using Ru nanoparticles showed no comparable selectivity. Furthermore, Ru nanoparticles supported on UiO-66 exhibited lower activity compared to the single-site RuH_2 species, indicating that the MOF-supported RuH_2 species are not only more selective but also more catalytically active. This also supports the conclusion that the active species are the intact RuH_2 complexes, rather than nanoparticles derived from MOF decomposition. Similar trends in size selectivity were observed when varying the pore sizes of Al-based MOFs supporting RuH_2 catalysts. These findings demonstrate both the thermal stability of MOFs under hydrogenolysis conditions and the ability of polymer chains to diffuse into the MOF pores, highlighting the potential of MOFs not merely as precursors or passive scaffolds, but as active materials that directly influence both the reactivity and selectivity of the depolymerisation process.

Other than polyolefins, hydrogenolysis can also be applied to polyesters. Using UiO-66, Farha and coworkers showed that PET can be depolymerised to TA and monomethyl terephthalate (MMT) under 1 atm of H_2, whilst producing ethylene and acetaldehyde from the ethylene glycol segment of the polymer.[27] Mechanistic studies suggest that UiO-66 first catalyses PET β-scission, forming carboxylic acids and vinyl-terminated units, the latter subsequently undergoing further hydrogenolysis to yield TA and ethylene (Fig 3B). During hydrogenolysis, UiO-66 converts to MIL-140A, which still possesses good, albeit slightly reduced activity. As such, reusability studies showed that product yields decreased after the first round of hydrogenolysis, with subsequent runs averaging 74% combined yield of TA and MMT with retention of MIL-140A's reactivity.

We note that, as discussed previously in the section on PET glycolysis, PET chains are highly immobile under typical reaction conditions. While the earlier study was conducted in ethylene glycol, the present hydrogenolysis study involves PET in the melt phase. Whether PET can effectively infiltrate the pores of UiO-66

or MIL-140A under these conditions remains an open question. Clarifying this point would be valuable for the field, as understanding whether depolymerisation occurs within the MOF pores or on the external surface is critical for guiding the rational design of MOF catalysts for PET depolymerisation. Techniques such as solid-state NMR or molecular modeling could be used to probe polymer-MOF interactions and provide insight into the accessibility of active sites during catalysis.

3.3. Pyrolysis

During pyrolysis, polymers are broken down at high temperatures in the absence of oxygen. Being tolerant to contamination, pyrolysis is one of the most industrially-viable methods for depolymerization. In addition to alkane production, pyrolysis can also transform polyolefins into unsaturated olefins and aromatics, unlike hydrogenolysis. In the only known study on MOF-catalysed plastic pyrolysis at the time of writing, UiO-66 containing missing linker defects, shown to be stable till 450 °C by TGA, was shown to efficiently catalyse pyrolysis of HDPE and LDPE.[13] Compared to control reactions performed in the absence of MOF, the UiO-66 elicited significantly increased yields of liquid fractions compared to solid waxes at 400 °C for 5 hours. Products in the liquid fraction mainly comprises of linear and cyclic alkanes and branched olefins. Compared to commercially-used Brønsted acidic zeolite catalysts which favour aromatic production,[7] the low yields of aromatics from UiO-66-catalysis suggests that it can potentially complement these zeolites in types of products formed.

The reaction was proposed to be catalysed by Lewis acidic, coordinatively unsaturated Zr sites located at the nodes of the UiO-66 framework. Polyethylene backbone scission is initiated through C–H activation at the UiO-66 node, forming Zr–alkyl complexes (Fig. 3C). This is followed by β-alkyl elimination, which results in C–C bond cleavage. The β-alkyl elimination step effectively reverses the migratory insertion that is the key step in the forward polymerisation of olefins. This proposed mechanism is distinct from that of zeolites,[7] which typically operate through Brønsted acid catalysed carbocationic pathways. The proposed mechanistic differences may also account for the distinct product distributions observed. Notably, UiO-66 samples synthesised with higher concentrations of missing linker defects, corresponding to a greater number of Lewis acidic sites, exhibited enhanced catalytic performance, yielding higher fractions of liquid products. This finding highlights the importance of defect engineering in modulating MOF reactivity and tuning depolymerisation pathways.

Additionally, the MOF's rigid framework stabilized and maintained the activity of the Zr nodes, preventing them from agglomeration that can result in loss of activity, as demonstrated where ZrO_2 microparticles were found to be inactive for PE pyrolysis under identical conditions. Extensive DSC analyses suggested that while HDPE was able to penetrate the MOF pores, the extensively-branched LDPE did not. Hence, it was likely that LDPE fragmentation first occurred on the MOF surface, forming shorter oligomeric fragments that could enter the pores for further cleavage. Despite prolonged heating at 400 °C for 5 hours, the UiO-66 MOFs could survive the pyrolysis process, with another subsequent round of reuse found to maintain overall conversions and liquid yields.

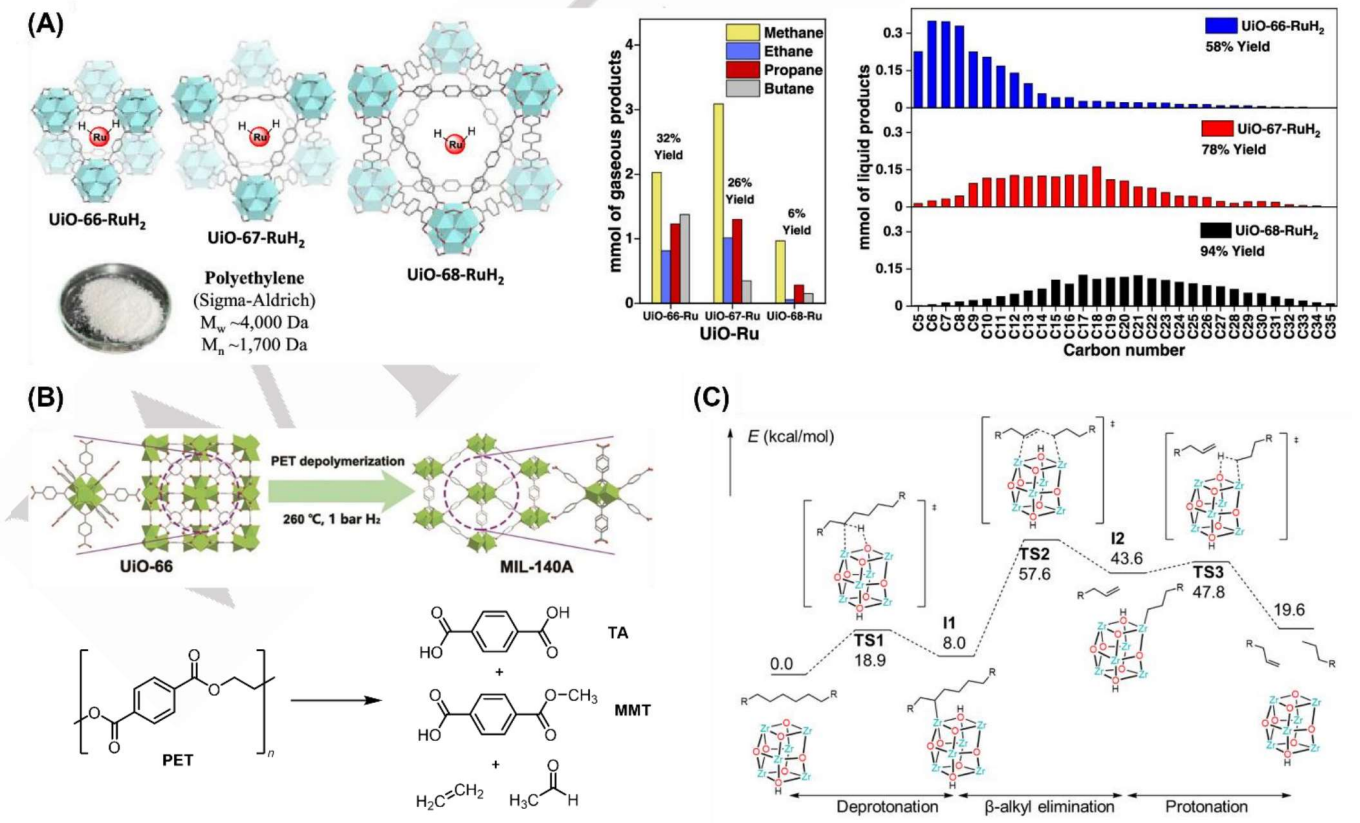

Figure 3. (A) Zr-based MOFs containing confined ruthenium hydrides with different pore sizes and the effects of shape-selective hydrogenolysis on the liquid product distributions from PE. Reproduced from ref. [11], Copyright (2023) American Chemical Society, CC-BY-NC-ND 4.0 (https://creativecommons.org/licenses/by-nc-nd/4.0/); (B) PET hydrogenolysis catalysed by UiO-66 which undergoes a phase transition to MIL-140A. Adapted with permission from ref. [21] .Copyright (2022)

Wiley-VCH; (C) Proposed mechanism for PE pyrolysis catalysed by the coordinatively-unsaturated nodes of UiO-66 MOFs with missing-linker defects. Adapted with permission from ref [13].Copyright (2024) Wiley-VCH.

3.4. Photocatalysis

Photocatalytic degradation of plastics is attractive for its low energy requirements, where catalyst activation results from irradiation, and can be performed at ambient aerobic conditions instead of requiring high temperatures unlike the aforementioned reactions. Due to the strongly oxidizing reactive intermediates generated, photocatalysis can depolymerize plastics containing cleavable bonds, as well as those with saturated C-C backbones.[43]

MOF-catalysed photocatalytic depolymerization can be performed by encapsulation of uniformly-dispersed nanoparticles within MOF structures with high thermal and chemical stability (e.g. UiO-66 and derivatives). Not only does the framework prevent nanoparticle aggregation, their well-defined pore dimensions can regulate the distribution and growth of nanoparticles within the pores that play direct roles in reactivity, and their porosity facilitates photon penetration for light absorption. Several strategies have been developed to synthesise these MOF-NP composites by post-synthetic modification: In one method, Zn^{2+} coordination with the amine groups in UiO-66-NH_2 [$Zr_6O_4(OH)_4(NH_2\text{-BDC})_6$], NH_2-BDC = 2-aminoterephthalate] allows its uniform distribution throughout the framework. Subsequently, partial calcination converts the Zn^{2+} into ultrasmall ZnO nanoparticles (2-7 nm) while maintaining UiO-66 framework integrity (Fig 4A).[22] Embedding ZnO into the MOF pore results in electronic synergy between both components, allowing interfacial charge transfer and redistribution upon photoirradiation that can bring about PLA and PVC degradation to acetic acid, whilst releasing H_2. Similarly, UiO-66 post-synthetically loaded with glucose can be subjected to mild pyrolysis at 240 °C to transform these guests into well-dispersed ultrasmall carbon nanodots (CDs) (~ 2 nm) embedded within the MOF pores (Fig 4B), that can efficiently upcycle PVC into acetic acid with light.[23] In an alternative to high-temperature MOF-NP synthesis, Zhang and coworkers demonstrate the possibility of synthesizing such composites through in-situ photoreactions (Fig 4C).[44] Fe-MOFs were first post-synthetically modified by partial replacement of Fe sites with Ag^+. After photoirradiation for 15 minutes, these Ag^+ sites are converted to Ag_2O nanoparticles, resulting in defect formation within the MOF structure that forms mesopores. These MOF composites could convert PEG, PET and PE microplastics to value-added chemicals such as formic and acetic acid, coupled with H_2 production. Notably, in these examples, the MOF-nanoparticle composite offers far superior catalytic performance compared to the MOF and NPs individually, signifying intimate mutual electronic influence when both components are in close interfacial contact upon NP confinement within MOF pores.

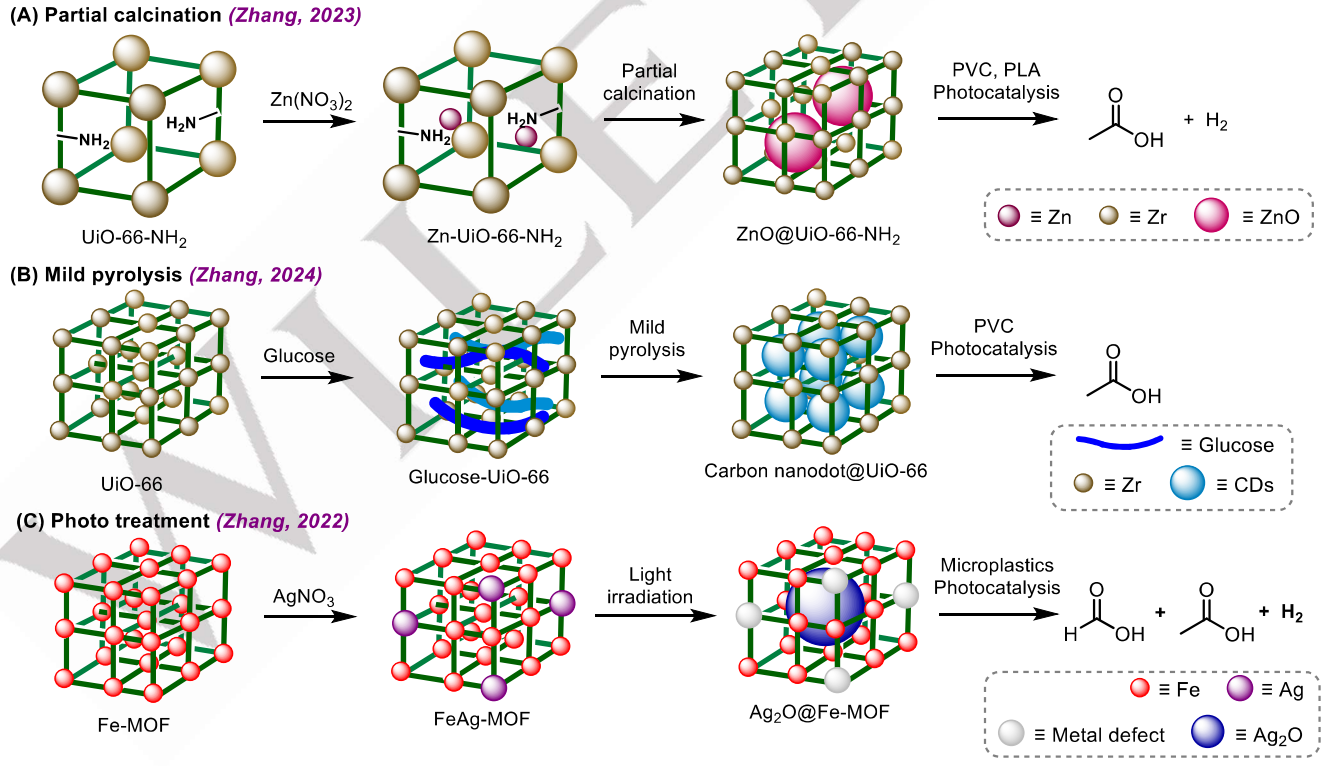

Figure 4. Schematic illustration showing the synthesis of MOF-NP composites for photocatalytic plastic degradation via (A) partial calcination of Zn^{2+}-containing UiO-66-NH_2;[22] (B) mild pyrolysis to transform glucose embedded in UiO-66 MOFs into CDs; [23] (C) In-situ photoreactions to convert Ag^+ sites in FeAg-MOFs to Ag_2O nanoparticles with the simultaneous creation of mesopores.[44]

3.5. Enzymatic Hydrolysis

In recent years, the potential of biocatalysis in depolymerization is beginning to be realized. Although PET hydrolysis has thus far been most extensively studied, enzymatic oxidative depolymerization of other recalcitrant plastics such as PEs are also witnessing considerable advances.[45] Catalysed by enzymes, reactions typically occur in aqueous environments at much lower temperatures than that required for many chemical depolymerization approaches, and can offer excellent product selectivity. However, biocatalysis typically occurs under homogeneous conditions, making enzyme recovery for reuse challenging and impractical, adding to the costs of large-scale PET degradation, Additionally, the enzymes can be susceptible to denaturation from salts, heat and mechanical forces. Composites of MOFs with enzymes offers a route towards heterogenization, facilitating recovery and reuse. In addition, encapsulation of enzymes within MOF pores can stabilize them against denaturation, with the MOF itself potentially even contributing towards depolymerization reactivity (vide infra).

Enzyme-MOF composites can be assembled by anchoring the enzymes to the external MOF surface, achieving enzyme heterogenization whilst retaining their accessibility for reaction with plastic substrates. For instance, *Candida rugosa* lipase (CrL) anchored on UiO-66-NH_2 could break down PET to BHET (Fig 5A).[24] Although several MOFs were investigated as supports (e.g. UiO-66, UiO-66-COOH, UiO-66-NO_2, MIL-125, MIL-100(Fe), ZnBDP) using BHET as a model substrate, UiO-66-NH_2 was chosen for enabling high surface enzyme attachment, excellent chemical and structural stability that allowed retention of crystallinity after CrL immobilization, and activity for BHET hydrolysis. Notably, PET degradation was only observed for the CrL-anchored MOF, and not when using CrL or UiO-66-NH_2 alone, which was attributed to preferential adhesion of the complex to the plastic that enhanced interfacial contact for hydrolysis.

Alternatively, enzymes encapsulated within MOF pores can still function effectively for PET degradation. Exploiting the excellent size complementary between *Humicola insolens* Cutinase (HiC) enzyme and NU-1000 [$Zr_6(O)_4(OH)_4(H_2O)_4(OH)_4(TBAPy)_2$], TBAPy = 1,3,6,8-tetrakis(p-benzoate)pyrene), HiC encapsulated within the MOF pores showed enhanced stability against denaturation, whilst extending enzyme utility through heterogenisation to allow multiple cycles of reuse.[25] The MOF-HiC composite showed enhanced hydrolytic activity in converting PET powder into TA and BHET, in contrast with HiC alone which was not active. This augmented reactivity was attributed to improved enzyme stability, with synergistic contributions of Nu-1000's Zr_6 nodes for hydrolysis. Using a similar concept, a multienzyme complex (MC) immobilized onto bimetallic Ca/Zn-containing imidazolate framework (CaZn-MOF) can stabilize the MC spatial conformations to enhance substrate adhesion and accessibility, allowing complete PET hydrolysis to TA.[26] Unlike the free MC, stability enhancement upon MOF immobilization allowed the MC@CaZn-MOF to be reused for 5 consecutive cycles of PET hydrolysis, retaining ~60% of its original activity.

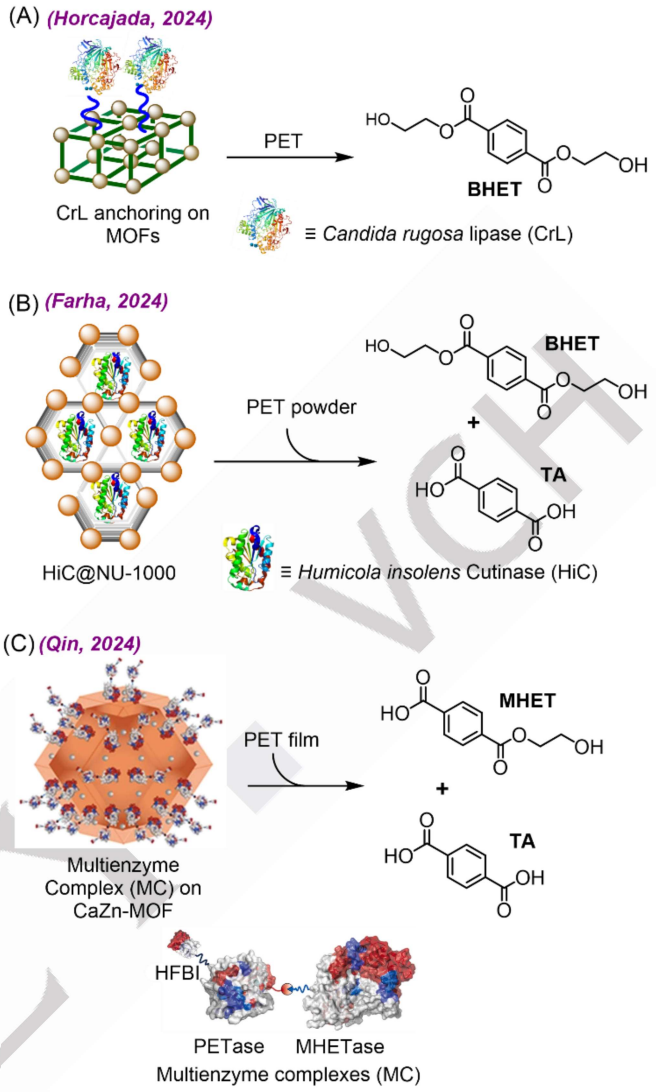

Figure 5. MOF-enzyme composites for biocatalytic PET hydrolysis: (A) by anchoring *Candida rugosa* lipase (CrL) on UiO-66-NH_2 [24]; (B) Encapsulation and stabilising *Humicola insolens* Cutinase in NU-1000 pores;[25] and (C) immobilisation of multi-enzyme complex onto bimetallic CaZn-MOF. Reprinted from ref [26]; Journal of Hazardous Materials, 477, Hui-Min Qin et. al., A customized self-assembled synergistic biocatalyst for plastic depolymerization, 135380, Copyright (2024), with permission from Elsevier.

3.6. Other Emerging Applications of MOFs in Depolymerisation

On top of the range of reactivity accessible for depolymerization, MOF catalysts can also be designed to harvest micro- and nanoplastics from wastewater and subsequently degrade them into harmless products for environmental remediation. In one strategy, electrostatic attractions between nano-sized Fe^{2+}-containing ZIF-8 MOFs (zeta potential ξ = +21 mV) and PET nanoplastics (ξ = -43 mV) brings about their abstraction, whereupon the MOF subsequently catalyses PET degradation by glycolysis.[46] Using a different strategy, MOF hydrophobicity was exploited for microplastic remediation, where Fe@ZIF-8 MOFs modulated with n-butylamine was shown to achieve 98% polystyrene microparticle removal, capitalizing on favourable hydrophobic-hydrophobic interactions between the nano-MOF

surfaces and PS.[46] Although not demonstrated for PS degradation, these Fe^{2+}-impregnated MOFs can be easily collected by magnetic separation to enable efficient microplastic removal.

Due to their excellent bottom-up designability and ease of achieving uniform metal dispersal within the framework, MOFs are also useful precursors for synthesizing carbon-support multimetallic catalysts, whose different metals contribute synergistically for plastic depolymerization. In one example, ZIF containing both Co^{2+} and Zn^{2+}, encapsulating a Mo precursor within the framework can be pyrolyzed to form a N-doped carbon supported bimetallic catalyst (CoMo@NC) after evaporation of Zn during pyrolysis.[47] CoMo@NC catalyses PET hydrogenolysis to afford TA in 91% within 10 h at 260°Cunder 1 atm H_2, which is far superior to the performance of the monometallic catalyst analogues. Both metals were shown to play synergistic roles, with Mo sites mainly eliciting initial PET β-scission, with the Co sites activating H_2 and subsequent hydrogenolysis of the intermediates.

4. Recommendations

MOFs have shown significant promise as catalysts for depolymerisation in the pioneering studies discussed in this review. To carry the field forward, we distill several best practices from these works that can guide future research and improve both the reliability and relevance of reported findings:

1) Post-reaction characterisation: To ensure that the reported catalytic performance can be attributed to the MOF structures rather than MOF-derived materials, comprehensive post-reaction characterisation should be routinely performed. Techniques such as X-ray diffraction, X-ray absorption spectroscopy, and electron microscopy can be used to confirm the structural integrity of the MOF and identify any framework degradation, including changes in polymorph or phase transitions. For systems employing single-atom catalysts or metalated nodes, it is particularly important to assess whether nanoparticle formation has occurred during the reaction. Catalyst reusability should also be tested over multiple cycles, with additional characterisation to monitor deactivation mechanisms and structural evolution. Furthermore, metal leaching should be assessed using elemental analysis (e.g. ICP-AES or ICP-MS) to verify that the observed activity does not arise from soluble species leached from the MOF.

2) A unique feature of MOF–polymer systems is the inherently low diffusivity of polymer chains into the MOF pores. As such, determining whether catalysis takes place within the pore or occurs primarily on the external surface is essential for evaluating the viability of MOFs as catalysts. As discussed in the introduction, techniques such as two-dimensional solid-state NMR, differential scanning calorimetry (DSC), and molecular modelling can offer valuable insights into polymer–MOF interactions and help elucidate the extent of polymer infiltration. These studies are especially critical when using MOFs with small pore apertures, such as ZIF-8 or even UiO-66, where polymer access to internal active sites may be significantly restricted.

3) Testing real post-consumer plastics: Real-world post-consumer plastics contain a wide range of additives, including but not limited to plasticizers, dyes and pigments, flame retardants, and fillers, all of which may interfere with MOF-based catalysis. Thus, testing solely on virgin plastic resins, which lack these components, may lead to an inaccurate assessment of catalyst performance and practical applicability.[48] For example, the presence of dyes is expected to have a significant impact on photocatalytic processes. Studies should thus include depolymerisation reactions using post-consumer plastic waste and compare the outcomes with those obtained from pure, additive-free materials. In addition, the molecular weight of commercial plastics is often substantially higher than that of resins or model compounds commonly used in catalytic studies. Higher molecular weight polymers exhibit significantly lower diffusivity, which can further limit access to active sites within the MOF. Future investigations should therefore ensure that catalysts are tested on high-molecular-weight polymers to more accurately reflect their performance in realistic depolymerisation scenarios.

4) Testing of mixed plastics streams: Building on the previous point, MOF catalysts must also be evaluated using mixed plastic streams to assess their practical viability. Physical sorting of plastics is costly and difficult to scale, and real-world waste streams typically contain a mixture of different polymers along with contaminants such as food residues and paper. For MOFs to be applicable in such contexts, they must demonstrate the ability to depolymerise target plastics in the presence of these common impurities. However, selective depolymerisation may offer a promising strategy for chemically separating mixed plastic waste. By leveraging the structural tunability of MOFs, it may be possible to design catalysts that preferentially depolymerise specific polymers while leaving others intact, enabling staged or sequential chemical recycling.

5) Comparison with best-in-class catalysts: MOFs possess several appealing features such as tunability, reticular design, and the potential for size-selective catalysis. However, their performance should be benchmarked against established catalytic systems, including homogeneous catalysts and other heterogeneous platforms such as zeolites, metal oxides, and metal nanoparticles. Identifying reactivities and product selectivties that are unique to MOFs or complementary to best-in-class alternatives will help establish the role of MOFs within the broader depolymerisation catalyst field.

5. Conclusions and Outlook

Our survey of MOF depolymerisation catalysts has demonstrated that they are promising platforms for recycling and upcycling some of the most common and recalcitrant petroleum-based plastics in production, especially the polyolefins and PET. Usage of archetypical MOFs that are thermally, chemically and/or hydrolytically stable has not only showcased their functional versatility, but also enable many of them to be reused for multiple cycles with retention of catalytic activity. Their stable framework structures enable porosity retention, stabilisation of catalytic sites from agglomeration, and also enable them to useful as nanoreactors to host nanoparticles and enzymes within their structures. Additionally, they can be used in water remediation for microplastic degradation, and their designability enables them to also function as precursors for synthesis of multimetallic heterogeneous catalysts whose different metal sites can exert synergistic reactivity in depolymerisation. Building on these extremely promising outcomes, MOFs are poised to play increasingly important roles in plastics recycling and upcycling in

coming years through the following key developments, ultimately contributing to greater materials circularity (Figure 6).

First, AI and automated high-throughput experimentation can be expected to feature prominently in expanding the MOF catalyst design space for depolymerisation, whilst taking into account practical considerations guiding MOF selection (Section 2). This not only accelerates screening of the vast MOF design space for catalyst discovery, but also potentially allows rapid optimisation of reaction conditions with considerable savings of manpower and physical resources. For instance, a deep neural network-based model was developed to predict optimal reaction conditions for Zn-BDC-catalysed PET glycolysis within 10 minutes with high fidelity, achieving <1% error between experiment and prediction for PET conversion and BHET yields.[37] In-silico catalyst design remains underexploited, though an early study using a DFT-based approach for designing homogeneous photoredox catalysts for PS oxidative upcycling may demonstrate the potential of this approach.[49] This will undoubtedly also include extending MOF catalyst design for new catalytic modalities such as electrocatalytic depolymerisation.

Second, new innovative solutions can be expected to improve MOF reusability and recycling for multiple cycles of depolymerisation. As material accumulation in MOF pores affects their reactivity, this naturally limits reusability and can add to the cost needed for frequent catalyst replacement. These issues are compounded by the fact that many MOFs are less thermally stable than traditional inorganic catalysts such as zeolites, which can be regenerated at high temperatures through calcination. To address this, there is growing interest in the regeneration and reconstruction of MOFs, akin to chemical or mechanical recycling. For instance, UiO-66 has been shown to undergo complete digestion in ammonium bicarbonate solution followed by successful reassembly, effectively enabling chemical recycling of the MOF.[50] This is particularly relevant for UiO-66-based catalysts used in pyrolysis and other Lewis acid-catalysed reactions. Other approaches include solvent-assisted thermal (SAT) regeneration, where low boiling point solvents are used to extract accumulated residues from the MOF pores,[51] as well as solvent-assisted mechano-regeneration.[52] Regeneration and reconstruction strategies are increasingly recognised as critical not only in catalysis but also in adsorption-related applications.[51] As the broader MOF community continues to develop practical regeneration techniques, depolymerisation-specific systems will likely benefit from these advances.

Additionally, there will be undoubtedly greater emphasis on developing MOF-catalysed depolymerisation methods that are tolerant to contaminants, which can take the form of other plastics, additives (e.g. dyes, plasticisers) and other non-plastics (e.g. metals, paper etc) typically found in municipal plastic waste. As highlighted in our recommended best practices, it is important to evaluate catalytic performance using real-world plastic streams that contain such additives and impurities. These components can significantly hinder access to MOF active sites or compete with plastic substrates via side reactions, ultimately reducing catalytic efficiency. Indeed, several classes of heterogeneous catalysts used in plastic depolymerisation are known to be vulnerable to deactivation by common additives. For example, metal-supported catalysts such as Ni/SiO_2 and Pt or Ru on zeolites are readily poisoned by aromatic stabilisers and amines.[48] It may be possible that MOFs featuring supported single-atom catalysts may exhibit similar vulnerabilities. Furthermore, acid-catalysed systems like zeolites are known to be susceptible to poisoning by amines, and we anticipate that acidic MOFs used to catalyst glycolysis or pyrolysis may face analogous challenges. Dyes are also known to hinder photocatalytic oxidation of plastics.[53] A systematic study on the interactions between various plastic additives and MOFs would therefore be valuable for advancing the field and guiding the design of more robust catalysts. At present, pyrolysis is amongst the most practical technologies for end-of-life treatment of plastic waste on large scales due to its tolerance for mixed plastic waste, though at the expense of product selectivity. One potential solution could selectively depolymerise plastics containing cleavable linkages, while not reacting with others present in the same mixture (e.g. polyolefins), enabling the monomers from the former to be separated from the latter. While this can be achieved with MOF catalysts for alcoholysis (Section 3.1), the ease of tuning MOF reactivity can be capitalised upon to engineer reactivity for one class of plastics over others, even with conditions that potentially can depolymerise multiple classes of plastics. For instance, UiO-66-catalysed hydrogenolysis for selective PET depolymerisation, whilst not affecting PE and PP contaminants present has been demonstrated.[27] The proven tolerance to contaminants will be of great value in improving the practicality of MOF-catalysed depolymerisation.

Finally, the unique designability and functional versatility of MOFs position them as promising platforms for sustainable and value-added depolymerisation for a range of recycling and upcycling processes, with potential for larger-scale industrial translation envisaged in coming years. Numerous scientific and engineering considerations are needed, which include reactor design (e.g. strategies to maintain high photon flux throughout the reaction vessel for photocatalysis), and batch-to-batch MOF catalyst consistency to ensure reproducibility for high turnovers. The latter includes ensuring uniform crystallite size, MOF surface area, as well as the nature and concentration of defects. Additionally, technoeconomic analyses will be critical to assess the economic feasibility of large-scale reactions. While methods to economically recover/ regenerate MOFs and feasibility for reactions on mixed plastics will lower the cost of depolymerisation, the cost of MOF catalyst production will also factor considerably. Compared to zeolites, which can cost approximately \$6/kg[54] for the common ZSM-5 used in PET depolymerisation, costs of MOFs such as UiO-66-NH_2 and MIL-160(Al) are higher and have been estimated to reach <\$20/kg on kiloton annual production scales using aqueous-based synthetic routes,[55] but further improvements to MOF synthesis protocols at scale can be expected to suppress production costs. In all, the potential of MOFs as emerging catalysts for depolymerisation is optimistic, with close collaboration between academia and industry necessary for achieving practical industrial adoption.

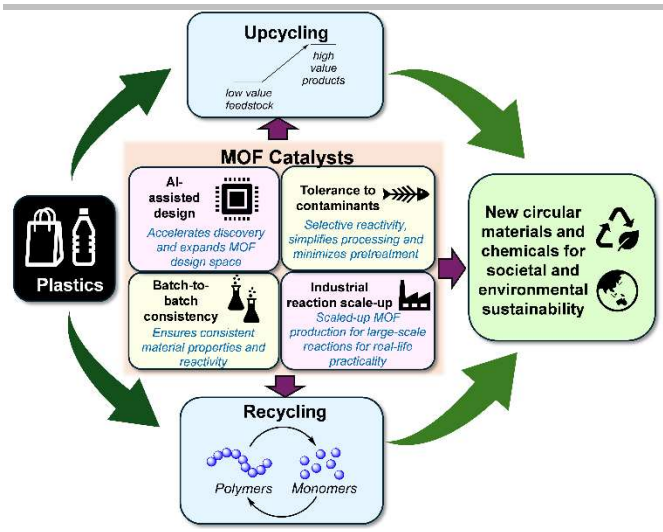

Figure 6. Key developments projected for MOF catalysts for plastics recycling and upcycling for a more sustainable materials future.

Acknowledgements

J.Y.C.L. acknowledges A*STAR and the NRF Fellowship (Award number: NRF-NRFF15-2023-0007) for financial support. S. Kitagawa and K. Otake are grateful for the support from Kyoto University's Overseas On-site Laboratory Program, and the financial support of KAKENHI, Grant-in-Aid for Scientific Research (S) (JP22H05005).

Keywords: Chemical recycling • upcycling • circular economy • plastics • heterogeneous catalysis

[1] a) K. Ragaert, L. Delva, K. Van Geem, *J. Waste Manag.* **2017**, *69*, 24-58; b) S. Yin, R. Tuladhar, F. Shi, R. A. Shanks, M. Combe, T. Collister, *Polym. Eng. Sci.* **2015**, *55*, 2899-2909.

[2] Ellen MacArthur Foundation, **2016**.

[3] *Vol. 2024*, International Union of Pure and Applied Chemistry, **2023**.

[4] a) C. Jehanno, J. W. Alty, M. Roosen, S. De Meester, A. P. Dove, E. Y. X. Chen, F. A. Leibfarth, H. Sardon, *Nature* **2022**, *603*, 803-814; b) A. Ong, J. Y. Q. Teo, Z. Feng, T. T. Y. Tan, J. Y. C. Lim, *ACS Sustainable Chem. Eng.* **2023**, *11*, 12514-12522; c) B.-N. T. Nguyen, J. Y. C. Lim, *Trends Chem.* **2024**, *6*, 100-114; d) J. Y. C. Lim, *ChemCatChem* **2025**, *17*, e202401626.

[5] aJ. Goyal, R. Verma, IHS Markit, **2021**; b) A. Bohre, P. R. Jadhao, K. Tripathi, K. K. Pant, B. Likozar, B. Saha, *ChemSusChem* **2023**, *16*, e202300142.

[6] a) C. Jehanno, M. M. Pérez-Madrigal, J. Demarteau, H. Sardon, A. P. Dove, *Polym Chem* **2019**, *10*, 172-186; b) K. V. Khopade, S. H. Chikkali, N. Barsu, *Cell Rep Phys Sci* **2023**, *4*, 101341.

[7] Z. Dong, W. Chen, K. Xu, Y. Liu, J. Wu, F. Zhang, *ACS Catal.* **2022**, *12*, 14882-14901.

[8] a) É. Casey, R. Breen, J. S. Gómez, A. P. M. Kentgens, G. Pareras, A. Rimola, J. D. Holmes, G. Collins, *ACS Sustainable Chem. Eng.* **2023**, *11*, 15544-15555; b) S. Su, L.-P. Xiao, X. Chen, S. Wang, X.-H. Chen, Y. Guo, S.-R. Zhai, *ChemSusChem* **2022**, *15*, e202200365.

[9] S. R. Shukla, V. Palekar, N. Pingale, *J. Appl. Polym. Sci.* **2008**, *110*, 501-506.

[10] O. M. Yaghi, M. O'Keeffe, N. W. Ockwig, H. K. Chae, M. Eddaoudi, J. Kim, *Nature* **2003**, *423*, 705-714.

[11] N. A. Manav Chauhan, Bharti Rana, Naved Akhtar, Chhaya Thadhani, Wahida Begum, and Kuntal Manna, *JACS Au.* **2023**, *3*, 3473−3484.

[12] S. Kitagawa, *Acc. Chem. Res.* **2017**, *50*, 514-516.

[13] T. T. Y. T. Jerry Zhi Xiong Heng, Xin Li, Wei Wei Loh, Yuting Chen, Zhenxiang Xing, Zhiyan Lim, Jennet Li Ying Ong, Katherine Shiyun Lin, Yusuke Nishiyama, Takefumi Yoshida, Lili Zhang, Ken-ichi Otake, Susumu Kitagawa, Xian Jun Loh, Enyi Ye, Jason Y.C. Lim, *Angew. Chem.* **2024**, *136*, e202408718.

[14] P. Europe, **2022**.

[15] J. Sun, J. Dong, L. Gao, Y.-Q. Zhao, H. Moon, S. L. Scott, *Chem Rev* **2024**, *124*, 9457-9579.

[16] Z. M. Patrycja Jutrzenka Trzebiatowska, Mateusz A. Baluk, Maria Gazda,, A. Z.-M. Arantxa Ecieza, *Appl. Surf. Sci.* **2024**, *673*, 160894.

[17] K. L. Nara Han, Jieun Lee, Jin Hui Jo, Eun Ji An, Gicheon Lee,, C. L. Won Seok Chi, *Chemosphere* **2024**, *364*, 143187.

[18] Q. Suo, J. Zi, Z. Bai, S. Qi, *Catal. Lett.* **2017**, *147*, 240-252.

[19] R.-X. Yang, Y.-T. Bieh, C. H. Chen, C.-Y. Hsu, Y. Kato, H. Yamamoto, C.-K. Tsung, K. C. W. Wu, *ACS Sustain. Chem. Eng.* **2021**, *9*, 6541-6550.

[20] M. Chauhan, C. Thadhani, B. Rana, P. Gupta, B. Ghosh, K. Manna, *Chem. Mater.* **2024**, *36*, 10670-10679.

[21] X. W. Yufang Wu, Kent O. Kirlikovali, Xinyi Gong, Ahmet Atilgan, Kaikai Ma,, N. C. G. Neil M. Schweitzer, Zhong Li, Xuan Zhang, and Omar K. Farha, *Angew. Chem. Int. Ed.* **2022**, *61*, e202117528.

[22] Y. D. Jibo Qin, Jianchi Zhou, Victor M. Candelario, Henrik Rasmus Andersen, Claus Hélix-Nielsen, and Wenjing Zhang, *Adv. Funct. Mater.* **2023**, *33*, 2214839.

[23] Y. D. Jibo Qin, Jianchi Zhou, Dan Zhao, Tobias Orlander,, C. H. e.-N. Henrik Rasmus Andersen, Wenjing Zhang, *Appl. Catal. B: Environ.* **2024**, *341*, 123355.

[24] T. H. Irene Rincon, Giacomo Armani, Sara Rojas, and Patricia Horcajada, *ChemSusChem* **2024**, e202301350.

[25] F. S. Audrianna Wu, Shengyi Su, and Omar K. Farha, *Chem. Bio. Eng.* **2024**.

[26] Y. H. Wei Zhang, Feng Yang, Lijun Guan, Fuping Lu, Shuhong Mao,, M. Y. Kangming Tian, Hui-Min Qin, *J. Hazard. Mater.* **2024**, *477*, 135380.

[27] Y. Wu, X. Wang, K. O. Kirlikovali, X. Gong, A. Atilgan, K. Ma, N. M. Schweitzer, N. C. Gianneschi, Z. Li, X. Zhang, O. K. Farha, *Angew. Chem. Int. Ed.* **2022**, *61*, e202117528.

[28] a) Y. An, X. Lv, W. Jiang, L. Wang, Y. Shi, X. Hang, H. Pang, *Green Chem. Eng.* **2024**, *5*, 187-204; b) C. Healy, K. M. Patil, B. H. Wilson, L. Hermanspahn, N. C. Harvey-Reid, B. I. Howard, C. Kleinjan, J. Kolien, F. Payet, S. G. Telfer, P. E. Kruger, T. D. Bennett, *Coord. Chem. Rev.* **2020**, *419*, 213388.

[29] S. Chavan, J. G. Vitillo, D. Gianolio, O. Zavorotynska, B. Civalleri, S. Jakobsen, M. H. Nilsen, L. Valenzano, C. Lamberti, K. P. Lillerud, S. Bordiga, *Phys. Chem. Chem. Phys.* **2012**, *14*, 1614-1626.

[30] B. Chen, X. Zeng, Y. Liu, F. Xiao, M. Huang, K. Bing Tan, D. Cai, J. Huang, G. Zhan, *Chem. Eng. J.* **2022**, *450*, 138470.

[31] P. Deria, W. Bury, J. T. Hupp, O. K. Farha, *Chem. Commun.* **2014**, *50*, 1965-1968.

[32] N. Hosono, T. Uemura, *Acc. Chem. Res.* **2021**, *54*, 3593-3603.

[33] N. Mizutani, N. Hosono, B. Le Ouay, T. Kitao, R. Matsuura, T. Kubo, T. Uemura, *J. Am. Chem. Soc.* **2020**, *142*, 3701-3705.

[34] D. Chakraborty, A. Yurdusen, G. Mouchaham, F. Nouar, C. Serre, *Adv. Funct. Mater.* **2024**, *34*, 2309089.

[35] E. Barnard, J. J. Rubio Arias, W. Thielemans, *Green Chem* **2021**, *23*, 3765-3789.

[36] G. Xi, M. Lu, C. Sun, *Polym. Degrad. Stab.* **2005**, *87*, 117-120.

[37] D. D. Pham, D.-N. Vo, M. T. Phong, H. H. Nguyen, T. Nguyen-Thoi, T.-P. T. Pham, D. Ha Le Phuong, L. K. H.

Pham, D. H. Won, D. L. T. Nguyen, T. M. Nguyen, *Chem. Eng. J.* **2024**, *490*, 151667.
[38] C. S. Tianlin Wang, Guangren Yu, Xiaochun Chen, *Fuel* **2021**, *304*, 121397.
[39] S. Baliga, W. T. Wong, *J. Polym. Sci. A Polym. Chem.* **1989**, *27*, 2071-2082.
[40] B. S. Rubin, *J Steroid Biochem Mol Biol* **2011**, *127*, 27-34.
[41] a) P. A. Kots, B. C. Vance, D. G. Vlachos, *React. Chem. Eng.* **2022**, *7*, 41-54; b) A. Ong, J. Y. Q. Teo, J. Y. C. Lim, *ACS Appl. Mater. Interfaces* **2024**.
[42] X. Wu, A. Tennakoon, R. Yappert, M. Esveld, M. S. Ferrandon, R. A. Hackler, A. M. LaPointe, A. Heyden, M. Delferro, B. Peters, A. D. Sadow, W. Huang, *J. Am. Chem. Soc.* **2022**, *144*, 5323-5334.
[43] J. Ran, A. Talebian-Kiakalaieh, S. Zhang, E. M. Hashem, M. Guo, S.-Z. Qiao, *Chem. Sci.* **2024**, *15*, 1611-1637.
[44] Y. D. Jibo Qin, Feiyan Wu, Yuechao Yao, Henrik Rasmus Andersen, Claus H´elix-Nielsen, Sung Yul Lim, Wenjing Zhang, *Appl. Catal. B: Environ.* **2022**, *319*, 121940.
[45] a) L. Shi, L. Zhu, *ChemBioChem* **2024**, *25*, e202300578; b) V. Tournier, S. Duquesne, F. Guillamot, H. Cramail, D. Taton, A. Marty, I. André, *Chem. Rev.* **2023**, *123*, 5612-5701.
[46] F. Pasanen, R. O. Fuller, F. Maya, *Chem. Eng. J.* **2024**, *490*, 151453.
[47] P. Wu, G. Lu, C. Cai, *Green Chem.* **2021**, *23*, 8666-8672.
[48] J. Ngu, S. Najmi, E. Selvam, B. Vance, P. Yang, D. G. Vlachos, *Nat Chem Eng* **2025**, *2*, 220-228.
[49] A. Ong, Z. C. Wong, K. L. O. Chin, W. W. Loh, M. H. Chua, S. J. Ang, J. Y. C. Lim, *Chem. Sci.* **2024**, *15*, 1061-1067.
[50] J. Chu, F.-S. Ke, Y. Wang, X. Feng, W. Chen, X. Ai, H. Yang, Y. Cao, *Commun Chem* **2020**, *3*, 5.
[51] L. Hashemi, M. Y. Masoomi, H. Garcia, *Coord. Chem. Rev.* **2022**, *472*, 214776.
[52] H. K. Lee, J. H. Lee, H. R. Moon, *Inorg. Chem.* **2021**, *60*, 11825-11829.
[53] S. Oh, E. E. Stache, *J. Am. Chem. Soc.* **2022**, *144*, 5745-5749.
[54] *Vol. 2025*, **2025**.
[55] a) H. Luo, F. Cheng, L. Huelsenbeck, N. Smith, *J. Environ. Chem. Eng.* **2021**, *9*, 105159; b) M. I. Severino, E. Gkaniatsou, F. Nouar, M. L. Pinto, C. Serre, *Faraday Discuss.* **2021**, *231*, 326-341.

Entry for the Table of Contents

This minireview discusses MOFs as emerging heterogeneous catalysts for plastic depolymerization. Leveraging their bottom-up designability, thermal stability, and high porosity, MOF catalysts are suitable for a range of different depolymerization reactions for the wide range of plastics currently available.

Institute and/or researcher Twitter usernames: ((optional))